

## Original Article

# Enhanced anticancer activity of Nanoformulation of Dasatinib against Triple-Negative Breast Cancer by reduced metabolic degradation

Fatemah Bahman <sup>1</sup>, Valeria Pittalà <sup>2,\*</sup>, Mohamed Haider <sup>3,4</sup>, Khaled Greish<sup>5,\*</sup>

<sup>1</sup> Department of Molecular Genetics, Kuwait Ministry of Health, Kuwait; [fato88.fb@gmail.com](mailto:fato88.fb@gmail.com)

<sup>2</sup> Department of Drug and Health Science, University of Catania, Italy; [valeria.pittala@unict.it](mailto:valeria.pittala@unict.it)

<sup>3</sup> Department of Pharmaceutics and Pharmaceutical Technology, College of Pharmacy, University of Sharjah, Sharjah, 27272, UAE; [mhaider@sharjah.ac.ae](mailto:mhaider@sharjah.ac.ae)

<sup>4</sup> Department of Pharmaceutics and Industrial Pharmacy, Faculty of Pharmacy, Cairo University, Cairo 71526, Egypt;

<sup>5</sup> Department of Molecular Medicine, and Nanomedicine Unit, Princess Al-Jawhara Center for Molecular Medicine, College of Medicine and Medical Sciences, Arabian Gulf University, Bahrain; [khaledfg@agu.edu.bh](mailto:khaledfg@agu.edu.bh)

\* Correspondence: [khaledfg@agu.edu.bh](mailto:khaledfg@agu.edu.bh); Tel.: +973 17237393; Fax: +9731 7246022. [valeria.pittala@unict.it](mailto:valeria.pittala@unict.it); Tel. +3909577384269

**Abstract:** Triple negative breast cancer (TNBC) is the most aggressive breast cancer accounting for around 15% of identified breast cancer cases. TNBC, by lacking estrogen receptor (ER), progesterone receptor (PR), and human epidermal growth factor receptor 2 (HER2), is unresponsive to current targeted therapies. Existing treatment relies on chemotherapeutic treatment but, despite an initial response to chemotherapy, the inception of resistance and relapse is unfortunately common. Dasatinib is an approved second-generation inhibitor of multiple tyrosine kinases and literature data strongly support its use in the management of TNBC. However, dasatinib binds to plasma proteins and undergoes extensive metabolism through oxidation and conjugation. To protect dasatinib from fast pharmacokinetic degradation and to prolong its activity, it was encapsulated on poly(styrene-co-maleic acid) (SMA) micelles. The obtained SMA-dasatinib nanoparticles (NPs) were evaluated for their physicochemical properties, *in vitro* antiproliferative activity in different TNBC cell lines, and *in vivo* anticancer activity in a syngeneic model of breast cancer. Obtained results showed that SMA-dasatinib is more potent against 4T1 TNBC tumor growth *in vivo* compared to free drug. This enhanced effect was ascribed to the encapsulation of the drug protecting it from a rapid metabolism. Our finding highlights the often-overlooked value of nanoformulations in protecting its cargo from degradation. Overall, results may provide an alternative therapeutic strategy for TNBC management.

**Keywords:** TNBC; dasatinib; poly(styrene-co-maleic acid) micelles; nanoformulation; metabolism; EPR; nanomedicine; targeted therapy.

## 1. Introduction

Breast cancer is the top widespread type of cancer among women in the U.S. and in 2021, it is estimated that 280,000 new cases, will be diagnosed with breast cancer [1,2]. The disease is globally affecting about 1 in 8 women in the U.S. during their lifetime. Breast cancer mortality could be attributed to metastasis by 80-90% [3].

Triple negative breast cancer (TNBC) is a long-lasting orphan disease and among the most clinically challenging breast cancer subtype. TNBC is the most aggressive and heterogeneous breast tumor that lacks all of three therapeutically relevant biomarkers including estrogen receptor (ER), progesterone receptor (PR), and human epidermal growth

factor receptor 2 (HER2) [4]. The conventional treatment for TNBC involves surgical excision and radiotherapy with a combination of adjuvant chemotherapies [5,6]. Despite current therapeutic regimens, patients affected by TNBC exhibit poor prognosis and are at high risk of early relapse and metastatic spread, as a result of resistance to chemotherapies [5]. Despite initially TNBC tends to be more chemo-sensitive than other groups of breast cancer, it shows high propensity to spread and metastasize to vital organs, for instance the lungs and brain rendering the survival rate still significantly lower than patients with non TNBC across any phase of diagnosis [7-9]. These aggressive phenotypes can be at least to some extent ascribed to the incidence of breast cancer stem cells (BCSCs). In addition, the lack of targeted therapies increases the use of traditional chemotherapy often accompanied by severe side-effects. The subclassification of TNBC based on gene expression profiling analysis includes mesenchymal (M), mesenchymal stem like (MSL), luminal androgen receptor positive (LAR), immunomodulatory (IM), basal like 1 (BL1) and basal-like 2 (BL2) [10-12]. This classification is paving the way to the identification of more specific molecular targets for TNBC treatment. In fact, these subtypes show different drug sensitivity profiles to anticancer treatments such as cisplatin for BL1 and BL2, PI3K and Proto-oncogene tyrosine-protein kinase (Src) inhibitors [13].

Src is a protein tyrosine kinase that regulates various cancerous events at an intracellular level, such as cellular adhesion, invasion, growth, survival, and vascular endothelial growth factor (VEGF) expression [14,15]. In addition, Src regulates an osteoclast function in normal bone and bone metastases [16]. A number of literature reports have evidenced in TNBC an abnormal activation and amplification of Src or Src-family kinases (SFK) and an involvement in metastasis regulation [17]. Not surprisingly TNBC shows an increased sensitivity to Src inhibitors compared to other cancer subgroups [18-20]. In addition, it has been demonstrated that ER and HER2 expression levels affect the beneficial effects of Src inhibitors in TNBC [21]. Therefore, Src can be considered as a new molecular target for TNBC therapy and Src inhibitors have long been proposed as new antitumoral treatments since they are able to prevent cell growth in liver, colon, breast, and ovarian cancers.

Dasatinib (Figure 1) is a Src, BCR-ABL, c-KIT, PDGFR- $\alpha$  and PDGFR- $\beta$ , and ephrin receptor kinase inhibitor approved by the Food and Drug Administration (FDA) for treating patients with Philadelphia chromosome positive leukemias (chronic myeloid leukemia; CML) [22,23]. Preclinical studies demonstrated significant inhibition of malignant breast cells growth through reducing the percentage of aldehyde dehydrogenase-positive (ALDH+) BCSCs within BL-2 subtype of breast cancer [13,24]. Considering that BCSCs are often responsible for the onset of chemotherapy resistance, dasatinib has been considered for the treatment of TNBC [24,25]. Similarly, preclinical studies evidenced synergistic or additive dasatinib activity with chemotherapy, implying that this Src inhibitor can offer clinical benefit in TNBC [26]. Regrettably, patients suffering from TNBC have inadequate benefit from Src inhibitors treatment [27-29]. In fact, despite promising preclinical results, a phase II clinical trial by administering dasatinib as a single agent highlighted only a 9% clinical benefit rate and other clinical trials terminated due to futility (e.g. NCT00817531, NCT00780676, etc.) [29]. Moreover, dasatinib suffer of some limitations related to its pharmacokinetic profile. Dasatinib is quickly absorbed with at least 80% of bioavailability of the oral dose; however, it is rapidly eliminated through CYP3A4-mediated metabolism, with a half-life of 3–4 h. In addition, dasatinib bioavailability is reduced by pH-modifying agents (antacids, H<sub>2</sub>-receptor blockers, proton pump inhibitors), and modified according to the concomitant treatment with CYP3A4 inducers or inhibitors [30].

In recent years considerable attention has been devoted to strategic application of nanoscience to pharmaceutical development with the aim of improving efficacy, delivery at the site of action, safety, physicochemical properties, and ADME (absorption, distribution, metabolism, and excretion) profile of bioactive compounds. In particular, nanoparticles formulations (NPs) can guarantee increased bioavailability of drugs administered orally, enhanced half-life of intravenous drugs (by reducing both metabolism and elimination), and augmented drug concentration in specific tissues. Taking in account dasatinib ADME profile, encapsulation of the drug into NPs may improve the drug efficacy,

minimize side-effects and permit the active principle to assemble at the malignant tumour site through the enhanced permeability and retention (EPR) effect [31,32]. In addition, using SMA micellar system to generate dasatinib NPs has multiple advantages over other nanoformulations. It generates a micelle with nearly neutral or slightly negative charge reducing opsonization of the micelles, recognition by the reticuloendothelial system and elimination from the blood circulation [33]. In this study, we encapsulated dasatinib into polystyrene co-maleic acid (SMA) micelles to generate micellar dasatinib system (SMA-dasatinib) that has been characterized for physicochemical properties including size, loading, charge, and release rate. In addition, SMA-dasatinib has been assessed for their anti-cancer effect *in vitro* using 4T1, MDA-MB-231, and MCF-7 cell lines and *in vivo* in a syngenic model of TNBC. Encouraging obtained results will pave the way for further study in the management of TNBC.

## 2. Materials and Methods

Dasatinib were retained from LC Laboratories (Woburn, Massachusetts, USA). Polystyrene co-maleic anhydride (molecular weight~1600), N-(3-dimethylaminopropyl)-N-ethylcarbodiimide hydrochloride (EDAC), Hank's balanced salt solution, Roswell Park Memorial Institute (RPMI) 1640 medium, fetal bovine serum (FBS), bovine serum albumin (BSA) and TrypLE express were bought from ThermoFisher Scientific (Dubai, UAE). L-glutamine, antibiotic solution of penicillin/streptomycin were purchased from (Merck Hertfordshire, UK). All consumable materials such as petri dishes, conical tubes (15 mL and 50 mL), cell culture flasks (25 cm<sup>2</sup> and 75 cm<sup>2</sup>), dialysis tubing were purchased from (Merck Hertfordshire, UK).

### 2.1. SMA-dasatinib micelles synthesis

SMA-micelles were synthesized as previously reported [34]. Briefly, SMA was hydrolyzed by dissolving the SMA powder in 1 M NaOH at 70 °C to reach a concentration of 10 mg/mL. Then, the solution of hydrolyzed SMA was adjusted to pH 5.0 and EDAC in a 1:1 weight ratio with SMA was dissolved in distilled water (DW). Dasatinib was dissolved in dimethyl sulfoxide (DMSO) at 25% weight ratio to SMA. EDAC was added to the SMA solution simultaneously with dasatinib until stable pH at 5.0 pH is obtained. Then, the pH was raised up to reach 11.0 and maintained till become stable. The pH was then lowered to 7.4 and the solution was filtered 4 times using a Millipore Labscale TFF system with a Pellicon XL 10 KDa cutoff membrane. Finally, the concentrated SMA-dasatinib micelles were frozen at -80°C and the following day lyophilized (5 mTorr and -52°C) to achieve a stable SMA-dasatinib powder.

### 2.2. SMA-dasatinib micelles characterization

The SMA micelles loading was determined by using three different samples of 1.0 mg/mL of SMA-dasatinib micelles dissolved in DMSO, for measuring absorbance at 320 nm of dasatinib to pre-prepared the standard curve of the free dasatinib intending to determine the weight ratio between the micelle and the loaded drug.

Size distribution and zeta potential determination of SMA-dasatinib micelles it was used a Malvern ZEN3600 Zetasizer Nano series (Malvern Instruments Inc., Westborough, MA, USA) by using 1 mg/mL of the SMA-dasatinib micelles dissolved in either double distilled water as a diluent for size measurement or for charge measurement. Then, to verify the release rate of free drug (dasatinib) from SMA micellar system, two separate experiments have been performed by measuring the release in PBS and in FBS. A 2 mg of the prepared micelles were dissolved in 2 mL of PBS or FBS, respectively, and inserted into a 10 kDa cutoff dialysis membrane that was submerged in 20 mL of PBS or FBS for 72 hours. At specified time points, the surrounding water was collected from outside the dialysis bag and replaced with PBS or FBS, and the absorbance measured at 320 nm.

### 2.3. Cell culture

4T1, MDA-MB-231 and MCF-7 cell lines were purchased from American Type Culture Collection (ATCC) (Manassas, VA, USA). RPMI medium supplemented with 5% fetal bovine serum (FBS) was used to culture the cell lines while being maintained in a humidified atmosphere at 37 °C, 5% CO<sub>2</sub>.

#### 2.3.1. *In vitro* anti-proliferative effect of dasatinib and SMA-dasatinib micelles

Cells were seeded in 96-well plates (density: 4T1 5×10<sup>3</sup>, MDA-MB-231 5×10<sup>3</sup>, MCF-7 5×10<sup>3</sup> cells/well, respectively) and incubated for 24 hours at 37 °C in 5% CO<sub>2</sub> and then treated with a different of concentrations of dasatinib 0 to 10 µM) or SMA-dasatinib (0 to 10 µM). The cytotoxicity was assessed after 48 h incubation using a sulforhodamine B (SRB) assay as described previously [35]. Cells were fixed using 10% trichloroacetic acid and stained with SRB. The cytotoxicity experiments were performed in triplicate (n=3). Then, the 50% growth inhibition (IC<sub>50</sub>) was assessed by using SRB assay after 48 h incubation. HepG-2 cells also were seeded at a density of 50,000 cells/cm<sup>2</sup> onto a 25cm<sup>2</sup> flask. Then cells were treated by various concentration of dasatinib and SMA-dasatinib. 24 hours after incubation, the supernatants were collected and diluted accordingly to retreat 4T1 cells. Data was represented as mean ± SD of three independent experiments of each cell lines.

#### 2.4. *In vivo* effect of free and micellar-dasatinib treatment

The Laboratory Animal Care Facility of the Arabian Gulf University (AGU), Bahrain, supplied the Female Balb/c mice (6-12 weeks old, mean weight 20-25 gm). All animals were kept under standard conditions including controlled temperature (25 °C), a 12 h light-dark cycle and had free access to food and drinking water *ad libitum*. All animal experiments were performed based on the rules and regulations of the Arabian Gulf University Animal Care Policy, and approved by the Research and Ethics Committee, REC approval No: G- E003-PI-04/17.

To propagate the tumor, female Balb/c mice (n=3) were injected with one million 4T1 mammary carcinoma cells in both sides (right and left side) of the mice back. The tumor then was collected and cut down into small pieces of average size 1-3 mm<sup>3</sup> in a sterile PBS to sustain tumor viability. Following this, 5 mice of each group were shaved, anesthetized, and inoculated with one small piece of the 4T1 tumor tissue subcutaneously. When the tumors reached 100 mm<sup>3</sup> in size, mice were randomly distributed into three groups n=5 in each group (negative control, dasatinib and SMA-dasatinib) subjected to drug treatment. Dasatinib was administered at a dose of 5 mg/kg via the tail vein, while SMA-dasatinib at a dose of 5 mg/kg (dasatinib equivalent dose) dissolved in PBS was given by IV injection. The first day of drug administration was set as day 0. Tumor volume was measured by manual caliber; the volume was estimated by using this formula:

$$V \text{ (mm}^3\text{)} = ((\text{transverse section (W)}^2 \times \text{longitudinal cross section (L)}) / 2).$$

Tumor volumes were normalized by using the initial tumor volume and represented as mean ± standard error of the mean (SEM). Also, the body weight of mice was measured every day and normalized daily for 10 days.

#### 2.5. *In vivo* biodistribution of dasatinib and SMA-dasatinib

Female Balb/c mice were implanted with 4T1 cell tumors (1-3 mm<sup>3</sup>) tumor size, bilaterally on the flanks. When tumors reached 100 mm<sup>3</sup>, mice were randomly distributed into two groups (4 animals per group). The animals were injected with either dasatinib or its equivalence in SMA-dasatinib at 50 mg/kg via the tail vein. Mice were euthanized 24 h after the treatment and organs were collected. Internal organs (heart, lungs, liver, spleen, and kidneys) and tumor tissue were analyzed for dasatinib content. SMA-dasatinib was extracted using the methodology previously described [36]. Briefly, tissues were minced, weighed and snapped frozen before being pulverized. Frozen tissue powder (1 mg) was re-suspended in 67% ethanol and 4 M HCl (1 mL). The suspension was incubated at 70 °C for 0.5 h, sonicated and centrifuged to extract dasatinib from tissue samples. Dasatinib content was determined by absorbance at 320 nm and compared to a dasatinib calibration

curve. Dasatinib content was normalized to the weight of tissue and to the total weight of the organs from which it was extracted.

2.6. Statistical analysis

The data of *in vitro* and *in vivo* experiments was evaluated using GraphPad prism software. Tumor size measurements in different treatment groups are expressed as group means  $\pm$  SEM. *In vitro* cytotoxicity experiments of dasatinib and SMA-dasatinib treatment groups are expressed as means  $\pm$  SD. The statistical significance of difference between groups were performed using two-tailed t-test. Statistical differences were considered significant if the P-value was  $<0.05$ .

3. Results

3.1. Synthesis and characterization of SMA-dasatinib

SMA-dasatinib was synthesized and characterized by a low critical micelle concentration (CMC) as previously described [34]. Furthermore, the structural variation of hydrophobic styrene and hydrophilic maleic groups stimulates the quick construction of SMA micelles and facilitates the encapsulation of dasatinib. The loading of SMA-dasatinib was 11.5 %, calculated as the weight ratio of the dasatinib over the total amount of SMA micelle weight. Micelles average size measuring showed that SMA-dasatinib micelles were 198 nm and polydispersity index (PDI) of 0.17 which determined by dynamic light scattering (DLS). As shown in Table 1, the zeta potential of SMA-dasatinib is near neutral with a value of 0.0035 mV which can sustain the micelle in the blood circulation for a long time by lowering the clearance by the reticuloendothelial system and allows accumulation in the tumor [37].

Thus, the average size of SMA-dasatinib is within the size range to facilitate its accumulation in tumor tissue by the effect of enhanced permeability and retention (EPR) [38]. Moreover, the release rate of the drug from the micelles was more efficient in an environment mimicking extracellular pH than in the blood (53% vs. 44%) following 96 h incubation).

Table 1. Characterization of SMA-dasatinib <sup>1</sup>.

Micelle	Recovery	Loading (wt/wt)	Size (nm)	PDI <sup>2</sup>	Zeta Potential (mV)
SMA-dasatinib	65%	11.5 %	198	0.17	-0.0035

<sup>1</sup> Data are shown as mean values  $\pm$  standard deviation (SD). Values are the mean of triplicate experiments; <sup>2</sup> PDI = polydispersity index.

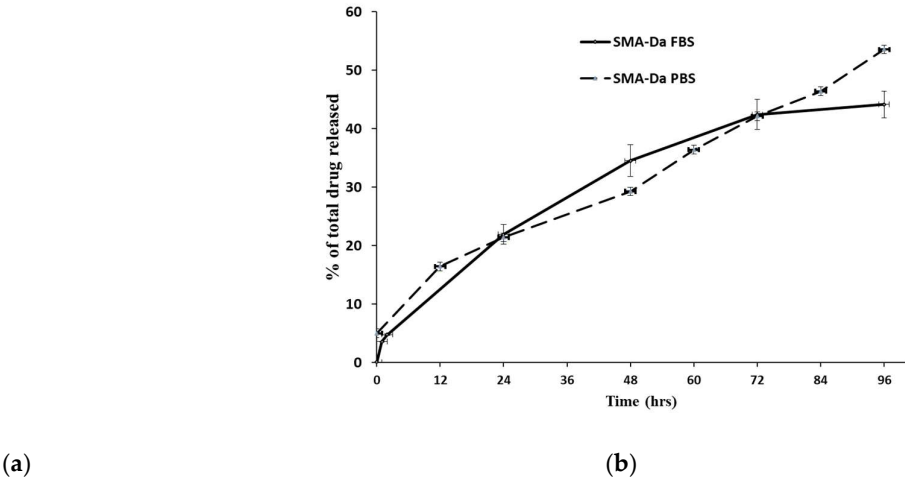


**Figure 1.** (a) Chemical structure of dasatinib; (b) SMA-dasatinib drug release studies. Cumulative release of dasatinib from SMA-dasatinib micelles at pH 7.4 in PBS and FBS. Data are presented as the average  $\pm$  SEM (n=3). 3.2. Drug release of SMA-dasatinib in vitro experiments

The release of dasatinib from SMA micelles was assessed at physiological pH 7.4 in PBS and FBS, respectively, for 96 h (Figure 1). The SMA-dasatinib micelles were stable in solution with about half of the formulation released after 96 h. moreover, first 2 h, the cumulative release was around 5% as shown in Figure 1. The stability of the micellar system depends on the slow release in the blood circulation which promotes the SMA-dasatinib accumulation at the tumor site through the EPR effect. A previous study has demonstrated the endocytosis of SMA micelle through caveolin-1 [39]. Therefore, SMA-dasatinib will be internalized by endocytosis and the release of dasatinib into the TNBC tumor cells.

### 3.3. Cytotoxicity of dasatinib and SMA-dasatinib versus breast cancer cell lines

The assessment of the effect of the cellular uptake of SMA-dasatinib and dasatinib on cell viability was achieved using different breast cancer cell lines, such as human MDA-MB-231, 4T1, and MCF-7 cells. The effect of dasatinib and SMA-dasatinib on cell viability was measured using SRB assay.

The treatment of MCF-7 cells (Figure 2A and Table 2) showed that both dasatinib and SMA-dasatinib had no significant difference in their cytotoxic profile after 48 h incubation and both displayed an  $IC_{50} > 10 \mu M$ . An  $IC_{50}$  value of  $6.1 \pm 2.2 \mu M$  was obtained for the dasatinib treatment of MDA-MB-231 cells while SMA-dasatinib exhibited an  $IC_{50}$  value of  $8.16 \pm 3.1 \mu M$  (Figure 2B and Table 2). Enhanced effect could be partially attributed to greater internalization capacity of MDA-MB-231 cells compared to MCF-7 cells [26]. 4T1 cells treated with free dasatinib and SMA-dasatinib showed a significant cytotoxic effect when compared to MCF-7 and MDA-MB-231 cells with  $IC_{50}$  of  $0.014 \pm 0.003$  and  $0.083 \pm 0.01 \mu M$ , respectively (Figure 2C and Table 2).

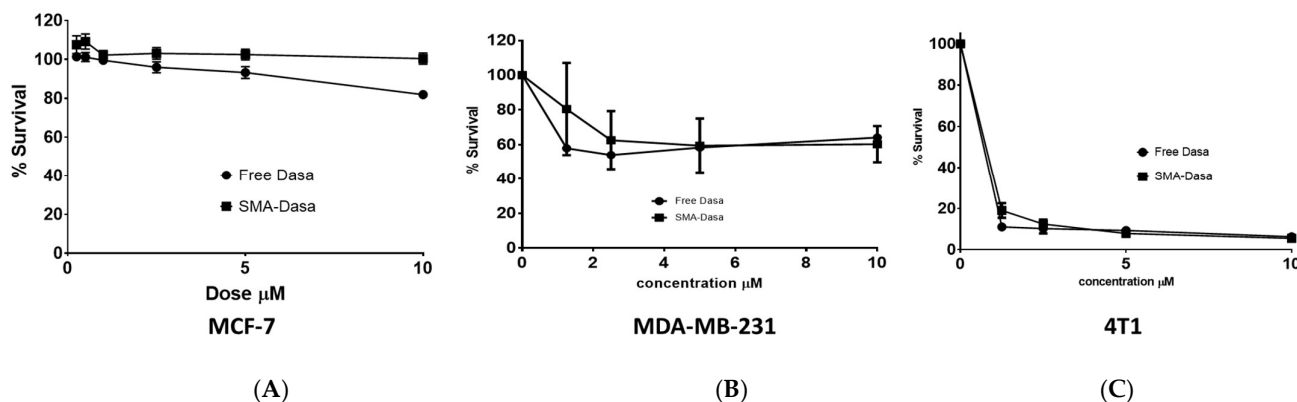


**Figure 2.** Cytotoxicity of dasatinib and SMA-dasatinib (A) against MCF-7, (B) MDA-MB-231, (C) and 4T1 cells. The cells were treated for 72 h with specific concentrations of dasatinib and SMA-dasatinib micelles. The cell number was determined using the SRB assay. Data are expressed as mean  $\pm$  SEM (n=3).

**Table 2.** Experimental  $IC_{50}$  values ( $\mu M$ ) of free dasatinib and SMA-dasatinib towards human MDA-MB-231, 4T1, and MCF-7 cells.

Cell line	IC <sub>50</sub> (μM) <sup>1</sup>	
	dasatinib	SMA-dasatinib
MCF7	>10	>10
MDA-MB-231	6.1 ±2.2	8.16 ±3.1
4T1	0.014 ±0.003	0.083 ±0.01
Hep-G2	>10	>10
4T1 after Hep-G2	0.21 ±0.04	0.09 ±0.012

<sup>1</sup> IC<sub>50</sub> value determination was performed using GraphPad Prism. Data are reported as IC<sub>3</sub> values in μM ± standard deviation (SD). Values are the mean of triplicate experiments.

### 3.3. Effect of dasatinib and SMA-dasatinib on the development of 4T1 tumors

The anticancer activity of dasatinib and SMA-dasatinib was evaluated using Balb/c mice harboring 4T1 tumor over a treatment period of 10 days. Figure 3A shows that during the first days' treatment with free dasatinib (5 mg/kg) tumor growth seems to be delayed while overall tumor size did not change significantly after 10 days in comparison to control treated mice. Very differently, treatment with SMA-dasatinib almost entirely stopped the tumor growth for the duration of the study.

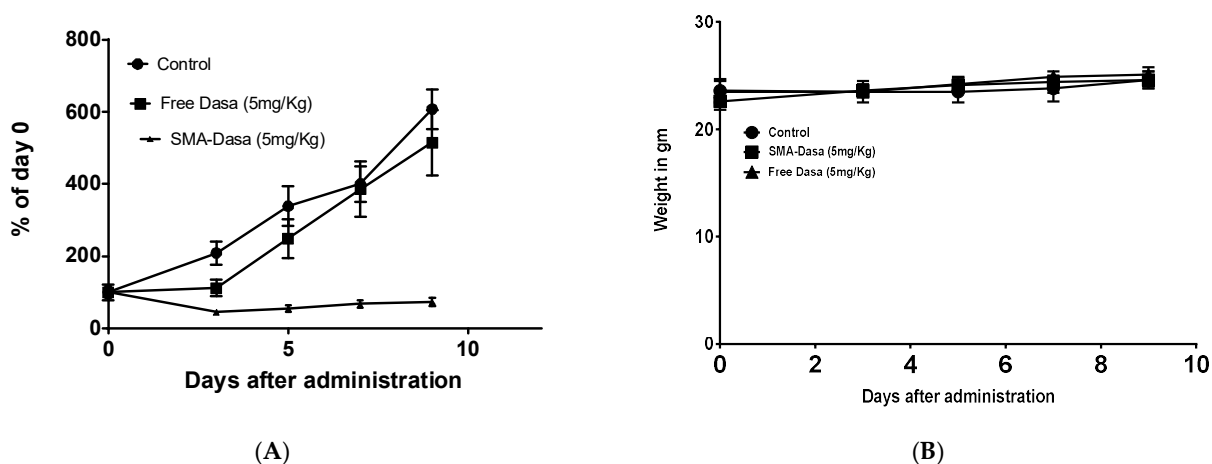


**Figure 3.** *In vivo* antitumor activity of dasatinib and SMA-dasatinib on 4T1 tumor bearing Balb/c mice. Mice were treated for 10 days with either dasatinib 5 mg/kg and SMA-dasatinib 5 mg/kg. Control group was injected with PBS (pH 7.4). Tumor volume changes (A) and body weight changes (B) were monitored over the treatment period. Data are presented as the mean of triplicate experiments ± standard error.

The therapeutic efficacy of dasatinib and SMA-dasatinib treatments were not associated with any statistically significant weight loss during the treatment period as shown in Figure 3B and Table 3.

**Table 3.** Body weight changes upon treatment with dasatinib and SMA-dasatinib were monitored over the treatment period <sup>1</sup>.

Day	Control	Dasatinib	SMA-dasatinib
0	23.5	23.5	22.6
9	24.6	25.1	24.6
Mean weight	23.8	24.2	23.9
Std. Deviation	0.4637	0.7537	0.7987

<sup>1</sup> Data are presented as the mean of triplicate experiments ± standard error.

### 3.3. *In vivo* biodistribution of dasatinib and SMA-dasatinib

The biodistribution of dasatinib and SMA-dasatinib were measured *in vivo*; to this extent, immunocompetent Balb/c mice harboring 4 T1 tumors were intravenously injected with equivalent doses of dasatinib or SMA-dasatinib and the concentration of dasatinib in various organs and tumor has been measured. As reported in Figure 4, dasatinib and SMA-dasatinib are distributed to the heart, liver, lung, kidney, and spleen. There was increased accumulation of dasatinib following SMA-dasatinib injection in spleen, kidney, and lung when compared to the free dasatinib injection (Figure 4A). No significant statistical difference was observed in the heart and liver. Also, in the tumor when comparing SMA-dasatinib to free dasatinib injection (Figure 4B) no statistically significant difference was observed.

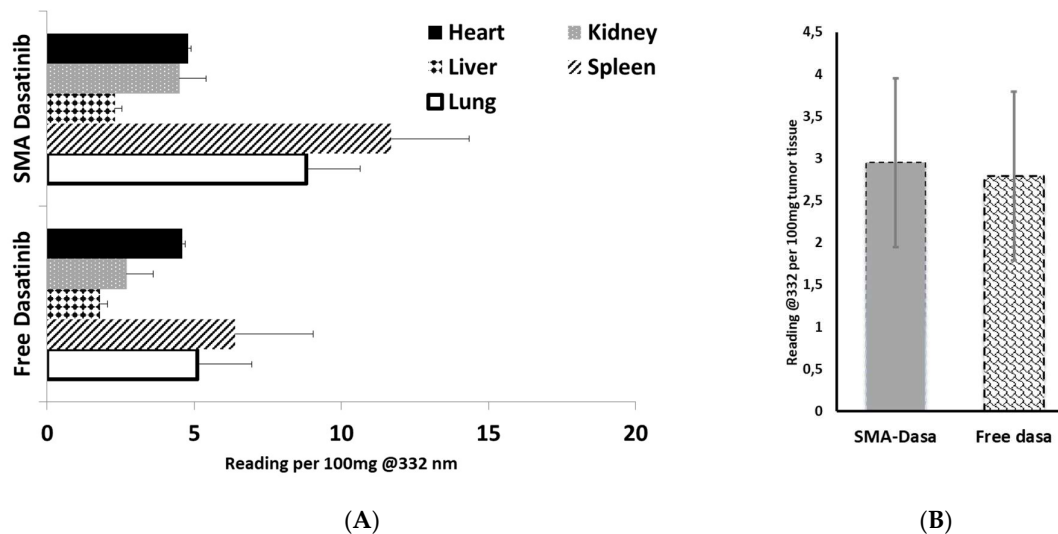


**Figure 4.** (A) Tissue and (B) tumor distribution of free dasatinib and SMA-dasatinib at 24 h after intravenous injection of dasatinib or SMA-dasatinib (50 mg/kg) to Balb/c mice bearing 4T1 tumors (n=5). Representation of the relative content of dasatinib per 100mg tissue expressed in free and micellar Dasatinib.

### 3.4. Cytotoxicity of dasatinib and SMA-dasatinib versus HepG2 cell line and 4T1 after passage in HepG2

The effect of SMA-dasatinib and dasatinib on HepG2 cell viability was assessed by using SRB assay. HepG2 cells upon treatment with dasatinib and SMA-dasatinib micelles did not show any significant toxicity (Figure 5A) after 48 h incubation and both displayed an  $IC_{50} > 10 \mu M$  (Table 2). However, when the supernatants obtained from HepG2 treatment with dasatinib and SMA-dasatinib, respectively, were added to 4T1 cells the correspondent  $IC_{50}$ s varied noticeably. While the SMA-dasatinib cytotoxicity did not change ( $IC_{50} = 0.09$  vs  $0.083 \mu M$ , respectively, Table 2); dasatinib cytotoxicity resulted in a 15-fold decrease of cytotoxicity ( $IC_{50} = 0.21$  vs  $0.014 \mu M$ , respectively, Table 2).

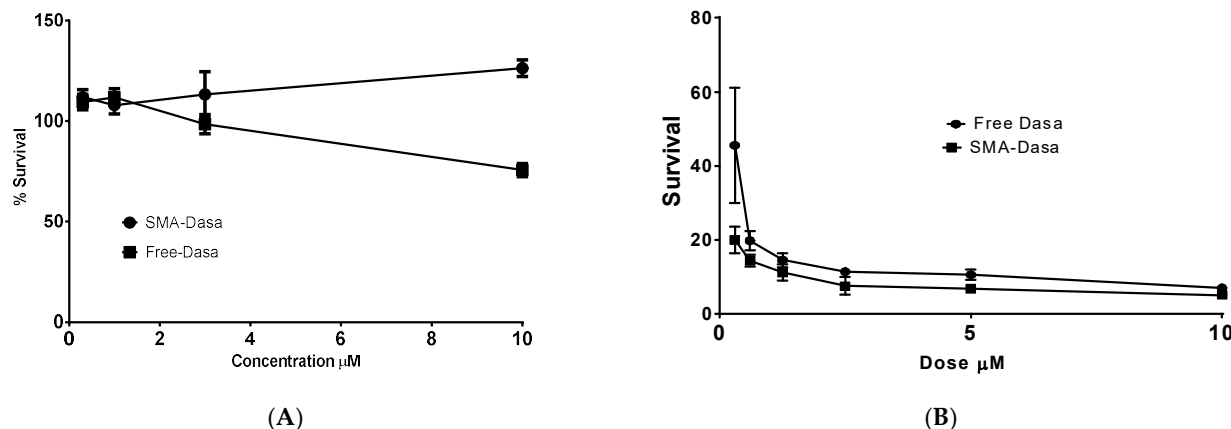


**Figure 5.** Cytotoxicity of dasatinib and SMA-dasatinib (A) against HepG2 cells, (B) 4T1 cells after treatment with HepG2. The cells were treated for 48 h with specific concentrations of dasatinib and SMA-dasatinib micelles. The cell number was determined using the SRB assay. Data are expressed as mean  $\pm$  SEM (n=8).

#### 4. Discussion

TNBC is a heterogeneous subtype that exhibits aggressive clinical behavior characterized by fast proliferation, chemoresistance, high recurrence risk, rapid progression, high probability of distant metastasis and low survival [40]. The main obstacles that hinder successful treatment is the absence of targetable hormonal receptors and prognosis biomarkers for the prediction and treatment of TNBC. Dasatinib is a multi-target kinase inhibitor, including BCR/ABL kinases and Src family kinases (SFK) that are closely linked to multiple signal pathways that regulate proliferation, invasion, survival, metastasis, and angiogenesis [41]. Dasatinib showed promising results in treatment of TNBC as a single agent or as a neoadjuvant; nevertheless, its use is limited by its poor aqueous solubility ( $6.49 \times 10^{-4}$  mg/mL). Moreover, after oral administration, dasatinib is subjected to extensive first pass metabolism where multiple CYP enzymes appear to have the potential to metabolize the drug [42]. Our current work aims at encapsulating dasatinib into SMA micelles to generate SMA-dasatinib micellar system that can improve its solubility in water, protect the drug against enzymatic degradation, potentiate its chemotherapeutic effect and minimize the rate of drug resistance.

The characterization of SMA-dasatinib micelles showed successful encapsulation of the drug with a loading capacity of 11.5%. Given that effective molecular size for EPR is 20-200 nm, the micellar size of 198 nm favors the accumulation of the nanoparticles in the tumor cells. In addition, the particle size of the prepared drug-loaded micelles should improve their circulation time and extend their plasma half-life by avoiding their rapid elimination from the kidney. The surface charge of the obtained prepared SMA-dasatinib micelles was almost neutral which is desirable to limit their interaction with active plasma constituents such as complement system and coagulation factors. Further, near neutral charge will ensure selective EPR-based extravasation through tumor vasculature with minimal interaction with normal endothelial cell membrane. The micellar formulations showed sustained slow-release rate of the drug for 96 h in both PBS and FBS (Figure 2), which shows that they can function as a reservoir for delivering a consistent level of dasatinib once concentrated extracellularly at tumor tissues and hence prolong the exposure of tumor cells to effective doses of the drug.

The examination of dasatinib-induced inhibition of metabolic activity on three commonly studied TNBC cell lines showed different responses. MCF7 cell line was the least sensitive to treatment with SMA-dasatinib and free drug ( $\text{IC}_{50} > 10 \mu\text{M}$ ) compared to MDA-MB-231 ( $\text{IC}_{50}$  8.16  $\mu\text{M}$  and 6.1  $\mu\text{M}$ , respectively). This correlates with previous studies that suggested that MDA-MB-231 are more sensitive due to the presence of active ABL kinase and their greater drug internalization capacity [26,43]. 4T1 cell line exhibited a

significantly high sensitivity to dasatinib and SMA-dasatinib ( $IC_{50} = 0.014 \mu M$  and  $0.083 \mu M$ , respectively) compared to MDA-MB-231 and MCF7 which may be due to their sensitivity to Src (Kin-2) receptor tyrosine kinase blockade [44]. Interestingly, there was no significant difference in the cytotoxic effect of the SMA-dasatinib and the free drug on the different types of TNBC cell lines *in vitro*. Nevertheless, Figure 4 showed that treatment with SMA-dasatinib significantly inhibited the tumor growth *in vivo* compared to animals treated with the free drug. Both treatments resulted in no significant weight loss in treated animals indicating that it is relatively safe to use dasatinib and SMA-dasatinib micelles in this animal model.

The biodistribution after IV administration showed a significantly high accumulation of SMA-dasatinib in the spleen compared to the free drug. This could possibly be due to the fact the size of SMA-dasatinib micelles is larger than the fenestration of the liver vasculature which can reduce the hepatic uptake of the micelles and may decrease the metabolism of the drug. On the other hand, there was no significant difference between the tumor distribution of dasatinib and SMA-dasatinib. Dasatinib is characterized by a large volume of distribution and human plasma proteins binding. *In vitro* studies showed that plasma protein binding of dasatinib can reach 96% creating a depot from which the drug is slowly released its free form. It may also increase the molecular size of the drug and enhance its accumulation at the tumor site by EPR effect similar to SMA-dasatinib [45].

Treatment of HepG2 cells with dasatinib and SMA-dasatinib micelles did not show significant toxicity ( $IC_{50} > 10 \mu M$ ). This is probably due to low expression levels of Src kinase, which reduced the sensitivity of the cell line to the drug [41]. The passage of dasatinib and SMA-dasatinib through HepG2 before treatment of 4T1 cells was carried out to check the effect of metabolism on the cytotoxic ability of the treatments. Dasatinib is significantly metabolized by CYP3A4 in the liver generating an active metabolite with similar potency to the drug, however it represents only 5% of dasatinib in plasma. The co-administration of potent CYP3A4 inducer results in a considerable reduction on  $C_{max}$  and AUC of the drug [42]. Treatment of 4T1 cells with supernatants obtained from HepG2 treatment showed a significant decrease in cytotoxicity of the free dasatinib while the cytotoxic effect of SMA-dasatinib remained unchanged. The encapsulation of dasatinib offered protection for the drug against enzymatic degradation. The size of the produced micelles enhanced its accumulation at the tumor site by EPR effect and reduced its liver uptake. Our work is an emphasis of the overlooked advantage of nano-delivery systems in term of cargo protection against degradation. This potential advantage was first described by Maeda back in 1991 [46]. Neocarzinostatin (NCS) is a very potent anticancer pretentious agent; however, NCS half-life is almost 1.9 minutes in tested mice. Using the nanoformulation of SMANCS protected the drug from the proteolytic activities in the plasma as well as extending its half-life by one order of magnitude. Overall, our work further emphasis the metabolic advantages of SMA-dasatinib nanosystems with a potential application for treating TNBC.

**Author Contributions:** Conceptualization, funding acquisition, project administration, supervision, writing—review and editing, K.G.; methodology, validation, F.B.; software, formal analysis, data curation, writing—original draft preparation, supervision, writing—review and editing, M.H., V.P.

**Funding:** This research was funded by Arabian Gulf University Research Grants to KG, Grant number G3-PI-04/17”.

**Institutional Review Board Statement:** All animal experiments were performed based on the rules and regulations of the Arabian Gulf University Animal Care Policy according to the guidelines of the Declaration of Helsinki, and approved by the Research and Ethics Committee, REC approval No: G- E003-PI-04/17.

**Acknowledgments:** We sincerely acknowledge the technical support of Ms Reem Al Zahrani and Dr. Sebastian Taurin.

## References

1. Siegel, R.L.; Miller, K.D.; Fuchs, H.E.; Jemal, A. Cancer Statistics, 2021. *CA: A Cancer Journal for Clinicians* **2021**, *71*, 7-33, doi:<https://doi.org/10.3322/caac.21654>.
2. Bray, F.; Ferlay, J.; Soerjomataram, I.; Siegel, R.L.; Torre, L.A.; Jemal, A. Global cancer statistics 2018: GLOBOCAN estimates of incidence and mortality worldwide for 36 cancers in 185 countries. *CA: A Cancer Journal for Clinicians* **2018**, *68*, 394-424, doi:<https://doi.org/10.3322/caac.21492>.
3. Chaffer, C.L.; Weinberg, R.A. A Perspective on Cancer Cell Metastasis. *Science* **2011**, *331*, 1559, doi:10.1126/science.1203543.
4. Hubalek, M.; Czech, T.; Müller, H. Biological Subtypes of Triple-Negative Breast Cancer. *Breast Care* **2017**, *12*, 8-14, doi:10.1159/000455820.
5. Waks, A.G.; Winer, E.P. Breast Cancer Treatment: A Review. *JAMA* **2019**, *321*, 288-300, doi:10.1001/jama.2018.19323.
6. Yagata, H.; Kajiura, Y.; Yamauchi, H. Current strategy for triple-negative breast cancer: appropriate combination of surgery, radiation, and chemotherapy. *Breast Cancer* **2011**, *18*, 165-173, doi:10.1007/s12282-011-0254-9.
7. Anders, C.; Carey, L.A. Understanding and treating triple-negative breast cancer. *Oncology (Williston Park)* **2008**, *22*, 1233-1239; discussion 1239-1240, 1243.
8. Yin, L.; Duan, J.-J.; Bian, X.-W.; Yu, S.-c. Triple-negative breast cancer molecular subtyping and treatment progress. *Breast Cancer Research* **2020**, *22*, 61, doi:10.1186/s13058-020-01296-5.
9. Yao, Y.; Chu, Y.; Xu, B.; Hu, Q.; Song, Q. Risk factors for distant metastasis of patients with primary triple-negative breast cancer. *Biosci Rep* **2019**, *39*, doi:10.1042/BSR20190288.
10. McLaughlin, R.P.; He, J.; van der Noord, V.E.; Redel, J.; Foekens, J.A.; Martens, J.W.M.; Smid, M.; Zhang, Y.; van de Water, B. A kinase inhibitor screen identifies a dual cdc7/CDK9 inhibitor to sensitise triple-negative breast cancer to EGFR-targeted therapy. *Breast Cancer Research* **2019**, *21*, 77, doi:10.1186/s13058-019-1161-9.
11. Wang, D.-Y.; Jiang, Z.; Ben-David, Y.; Woodgett, J.R.; Zacksenhaus, E. Molecular stratification within triple-negative breast cancer subtypes. *Scientific Reports* **2019**, *9*, 19107, doi:10.1038/s41598-019-55710-w.
12. Perou, C.M. Molecular stratification of triple-negative breast cancers. *Oncologist* **2010**, *15 Suppl 5*, 39-48, doi:10.1634/theoncologist.2010-S5-39.
13. Lehmann, B.D.; Bauer, J.A.; Chen, X.; Sanders, M.E.; Chakravarthy, A.B.; Shyr, Y.; Pietenpol, J.A. Identification of human triple-negative breast cancer subtypes and preclinical models for selection of targeted therapies. *J Clin Invest* **2011**, *121*, 2750-2767, doi:10.1172/jci45014.
14. Yeatman, T.J. A renaissance for SRC. *Nature Reviews Cancer* **2004**, *4*, 470-480, doi:10.1038/nrc1366.
15. Finn, R.S. Targeting Src in breast cancer. *Ann Oncol* **2008**, *19*, 1379-1386, doi:10.1093/annonc/mdn291.
16. Araujo, J.; Logothetis, C. Targeting Src signaling in metastatic bone disease. *Int J Cancer* **2009**, *124*, 1-6, doi:10.1002/ijc.23998.
17. Thakur, R.; Trivedi, R.; Rastogi, N.; Singh, M.; Mishra, D.P. Inhibition of STAT3, FAK and Src mediated signaling reduces cancer stem cell load, tumorigenic potential and metastasis in breast cancer. *Sci Rep* **2015**, *5*, 10194, doi:10.1038/srep10194.
18. Wheeler, D.L.; Iida, M.; Dunn, E.F. The role of Src in solid tumors. *The oncologist* **2009**, *14*, 667-678, doi:10.1634/theoncologist.2009-0009.
19. Ahluwalia, M.S.; de Groot, J.; Liu, W.M.; Gladson, C.L. Targeting SRC in glioblastoma tumors and brain metastases: rationale and preclinical studies. *Cancer Lett* **2010**, *298*, 139-149, doi:10.1016/j.canlet.2010.08.014.
20. Summy, J.M.; Gallick, G.E. Src family kinases in tumor progression and metastasis. *Cancer Metastasis Rev* **2003**, *22*, 337-358, doi:10.1023/a:1023772912750.
21. Fan, P.; McDaniel, R.E.; Kim, H.R.; Clagett, D.; Haddad, B.; Jordan, V.C. Modulating therapeutic effects of the c-Src inhibitor via oestrogen receptor and human epidermal growth factor receptor 2 in breast cancer cell lines. *Eur J Cancer* **2012**, *48*, 3488-3498, doi:10.1016/j.ejca.2012.04.020.

22. Steinberg, M. Dasatinib: a tyrosine kinase inhibitor for the treatment of chronic myelogenous leukemia and philadelphia chromosome-positive acute lymphoblastic leukemia. *Clin Ther* **2007**, *29*, 2289-2308, doi:10.1016/j.clinthera.2007.11.005.
23. Brave, M.; Goodman, V.; Kaminskas, E.; Farrell, A.; Timmer, W.; Pope, S.; Harapanhalli, R.; Saber, H.; Morse, D.; Bullock, J.; et al. Sprycel for chronic myeloid leukemia and Philadelphia chromosome-positive acute lymphoblastic leukemia resistant to or intolerant of imatinib mesylate. *Clin Cancer Res* **2008**, *14*, 352-359, doi:10.1158/1078-0432.Ccr-07-4175.
24. Kurebayashi, J.; Kanomata, N.; Moriya, T.; Kozuka, Y.; Watanabe, M.; Sonoo, H. Preferential antitumor effect of the Src inhibitor dasatinib associated with a decreased proportion of aldehyde dehydrogenase 1-positive cells in breast cancer cells of the basal B subtype. *BMC Cancer* **2010**, *10*, 568, doi:10.1186/1471-2407-10-568.
25. Tian, J.; Raffa, F.A.; Dai, M.; Moamer, A.; Khadang, B.; Hachim, I.Y.; Bakdounes, K.; Ali, S.; Jean-Claude, B.; Lebrun, J.-J. Dasatinib sensitises triple negative breast cancer cells to chemotherapy by targeting breast cancer stem cells. *British Journal of Cancer* **2018**, *119*, 1495-1507, doi:10.1038/s41416-018-0287-3.
26. Pichot, C.S.; Hartig, S.M.; Xia, L.; Arvanitis, C.; Monisvais, D.; Lee, F.Y.; Frost, J.A.; Corey, S.J. Dasatinib synergizes with doxorubicin to block growth, migration, and invasion of breast cancer cells. *Br J Cancer* **2009**, *101*, 38-47, doi:10.1038/sj.bjc.6605101.
27. Gucalp, A.; Sparano, J.A.; Caravelli, J.; Santamauro, J.; Patil, S.; Abbruzzi, A.; Pellegrino, C.; Bromberg, J.; Dang, C.; Theodoulou, M.; et al. Phase II trial of saracatinib (AZD0530), an oral SRC-inhibitor for the treatment of patients with hormone receptor-negative metastatic breast cancer. *Clin Breast Cancer* **2011**, *11*, 306-311, doi:10.1016/j.clbc.2011.03.021.
28. Campone, M.; Bondarenko, I.; Brincat, S.; Hotko, Y.; Munster, P.N.; Chmielowska, E.; Fumoleau, P.; Ward, R.; Bardy-Bouxin, N.; Leip, E.; et al. Phase II study of single-agent bosutinib, a Src/Abl tyrosine kinase inhibitor, in patients with locally advanced or metastatic breast cancer pretreated with chemotherapy. *Ann Oncol* **2012**, *23*, 610-617, doi:10.1093/annonc/mdr261.
29. Finn, R.S.; Bengala, C.; Ibrahim, N.; Roché, H.; Sparano, J.; Strauss, L.C.; Fairchild, J.; Sy, O.; Goldstein, L.J. Dasatinib as a single agent in triple-negative breast cancer: results of an open-label phase 2 study. *Clin Cancer Res* **2011**, *17*, 6905-6913, doi:10.1158/1078-0432.Ccr-11-0288.
30. Levêque, D.; Becker, G.; Bilger, K.; Natarajan-Amé, S. Clinical Pharmacokinetics and Pharmacodynamics of Dasatinib. *Clinical Pharmacokinetics* **2020**, *59*, 849-856, doi:10.1007/s40262-020-00872-4.
31. Qian, X.-L.; Zhang, J.; Li, P.-Z.; Lang, R.-G.; Li, W.-D.; Sun, H.; Liu, F.-F.; Guo, X.-J.; Gu, F.; Fu, L. Dasatinib inhibits c-src phosphorylation and prevents the proliferation of Triple-Negative Breast Cancer (TNBC) cells which overexpress Syndecan-Binding Protein (SDCBP). *PLoS One* **2017**, *12*, e0171169-e0171169, doi:10.1371/journal.pone.0171169.
32. Maeda, H.; Nakamura, H.; Fang, J. The EPR effect for macromolecular drug delivery to solid tumors: Improvement of tumor uptake, lowering of systemic toxicity, and distinct tumor imaging in vivo. *Adv Drug Deliv Rev* **2013**, *65*, 71-79, doi:10.1016/j.addr.2012.10.002.
33. Greish, K.; Fang, J.; Inutsuka, T.; Nagamitsu, A.; Maeda, H. Macromolecular therapeutics: advantages and prospects with special emphasis on solid tumour targeting. *Clin Pharmacokinet* **2003**, *42*, 1089-1105, doi:10.2165/00003088-200342130-00002.
34. Greish, K.; Jasim, A.; Parayath, N.; Abdelghany, S.; Alkhateeb, A.; Taurin, S.; Nehoff, H. Micellar formulations of Crizotinib and Dasatinib in the management of glioblastoma multiforme. *J Drug Target* **2018**, *26*, 692-708, doi:10.1080/1061186x.2017.1419357.
35. Vichai, V.; Kirtikara, K. Sulforhodamine B colorimetric assay for cytotoxicity screening. *Nat Protoc* **2006**, *1*, 1112-1116, doi:10.1038/nprot.2006.179.
36. Greish, K.; Fateel, M.; Abdelghany, S.; Rachel, N.; Alimoradi, H.; Bakhiet, M.; Alsaie, A. Sildenafil citrate improves the delivery and anticancer activity of doxorubicin formulations in a mouse model of breast cancer. *J Drug Target* **2018**, *26*, 610-615, doi:10.1080/1061186x.2017.1405427.

- 
37. Davis, M.E.; Chen, Z.; Shin, D.M. Nanoparticle therapeutics: an emerging treatment modality for cancer. *Nature Reviews Drug Discovery* **2008**, *7*, 771-782, doi:10.1038/nrd2614.
  38. He, C.; Hu, Y.; Yin, L.; Tang, C.; Yin, C. Effects of particle size and surface charge on cellular uptake and biodistribution of polymeric nanoparticles. *Biomaterials* **2010**, *31*, 3657-3666, doi:<https://doi.org/10.1016/j.biomaterials.2010.01.065>.
  39. Nehoff, H.; Parayath, N.N.; Domanovitch, L.; Taurin, S.; Greish, K. Nanomedicine for drug targeting: strategies beyond the enhanced permeability and retention effect. *Int J Nanomedicine* **2014**, *9*, 2539-2555, doi:10.2147/IJN.S47129.
  40. Dent, R.; Trudeau, M.; Pritchard, K.I.; Hanna, W.M.; Kahn, H.K.; Sawka, C.A.; Lickley, L.A.; Rawlinson, E.; Sun, P.; Narod, S.A. Triple-negative breast cancer: clinical features and patterns of recurrence. *Clin Cancer Res* **2007**, *13*, 4429-4434, doi:10.1158/1078-0432.Ccr-06-3045.
  41. Chang, A.Y.; Wang, M. Molecular mechanisms of action and potential biomarkers of growth inhibition of dasatinib (BMS-354825) on hepatocellular carcinoma cells. *BMC Cancer* **2013**, *13*, 267, doi:10.1186/1471-2407-13-267.
  42. Duckett, D.R.; Cameron, M.D. Metabolism considerations for kinase inhibitors in cancer treatment. *Expert Opin Drug Metab Toxicol* **2010**, *6*, 1175-1193, doi:10.1517/17425255.2010.506873.
  43. Huang, F.; Reeves, K.; Han, X.; Fairchild, C.; Platero, S.; Wong, T.W.; Lee, F.; Shaw, P.; Clark, E. Identification of candidate molecular markers predicting sensitivity in solid tumors to dasatinib: rationale for patient selection. *Cancer Res* **2007**, *67*, 2226-2238, doi:10.1158/0008-5472.Can-06-3633.
  44. Rao, S.; Larroque-Lombard, A.L.; Peyrard, L.; Thauvin, C.; Rachid, Z.; Williams, C.; Jean-Claude, B.J. Target modulation by a kinase inhibitor engineered to induce a tandem blockade of the epidermal growth factor receptor (EGFR) and c-Src: the concept of type III combi-targeting. *PLoS One* **2015**, *10*, e0117215, doi:10.1371/journal.pone.0117215.
  45. Kamath, A.V.; Wang, J.; Lee, F.Y.; Marathe, P.H. Preclinical pharmacokinetics and in vitro metabolism of dasatinib (BMS-354825): a potent oral multi-targeted kinase inhibitor against SRC and BCR-ABL. *Cancer Chemother Pharmacol* **2008**, *61*, 365-376, doi:10.1007/s00280-007-0478-8.
  46. Maeda, H. SMANCS and polymer-conjugated macromolecular drugs: advantages in cancer chemotherapy. *Advanced Drug Delivery Reviews* **1991**, *6*, 181-202, doi:[https://doi.org/10.1016/0169-409X\(91\)90040-J](https://doi.org/10.1016/0169-409X(91)90040-J).